

# Nitrogenation of Fe-Al Alloys. III: Absorption of Hydrogen in Nitrogenated Fe-Al Alloys

H. H. PODGURSKI AND R. A. ORIANI

Nitrogenation of Fe-2 pct Al alloys produces a large number of AlN particles and a large density of dislocations in the ferrite. We have measured the amount of nitrogen absorbed reversibly as a function of nitrogen activity at 500°C by alloys nitrogenated under different conditions. We have also measured the reversible hydrogen absorption at room temperature as a function of hydrogen fugacity and with varying amounts of preadsorbed nitrogen. Some preparative treatments produce some AlN-ferrite interface that can reversibly adsorb nitrogen at 500°C and hydrogen at 24.5°C upon sites not occupied by nitrogen. In the absence of such interface, the nitrogen absorption isotherms and the nitrogen-free hydrogen absorption isotherms are adequately described by a model based upon the thermodynamics of stressed bodies. However, the observed decrease of absorbed hydrogen caused by preadsorbed nitrogen is not explicable by the simple idea that a site occupied by nitrogen is unavailable to hydrogen.

IN Part II of this series<sup>1</sup> we showed that nitrogenated Fe-Al alloys, consisting of numerous, extremely small AlN particles and of ferrite phase containing a very large density of dislocations, absorb considerable amounts of nitrogen in excess of the normal lattice solubility. Part of the excess nitrogen was identified as being adsorbed at the AlN-ferrite interface, and another part was characterized as being held at the cores and associated stress fields of dislocations. The dislocation-held nitrogen was experimentally shown to exhibit reversible isotherms at various temperatures, and Li and Chou<sup>1a</sup> demonstrated remarkably good agreement between the experimental isotherms and isotherms calculated from the thermodynamics of stressed bodies.<sup>2</sup>

It is clearly of interest to investigate the extent and the manner of the lower-temperature absorption of hydrogen at various fugacities by nitrogenated alloys containing different, known amounts of absorbed nitrogen corresponding to measured activities. The initial idea was that the preadsorbed nitrogen would preempt dislocation-core sites from occupancy by hydrogen at room temperature, but that interference by nitrogen would be negligible away from the cores. The present investigation consists of nitrogenating an Fe-2 pct (by weight) aluminum alloy, establishing the reversible nitrogen content-activity isotherm at 500°C, and establishing the room-temperature reversible hydrogen content-fugacity isotherms for alloys with various amounts of frozen-in nitrogen, which at 500°C is reversibly absorbed. We compare the experimental nitrogen isotherms with isotherms calculated by the Li-Chou procedure, and the experimental hydrogen isotherms and isobars with curves calculated by the Li-Chou technique but modified to account for sites preempted by nitrogen.

## EXPERIMENTAL DETAILS AND RESULTS

### A) Nitrogenation and Nitrogen Isotherms

In order to produce alloys with different dislocation densities, both the nitrogenating conditions and the con-

H. H. PODGURSKI and R. A. ORIANI are with the U.S. Steel Research Laboratory, Monroeville, Pa.

Manuscript submitted November 8, 1971.

ditions for the subsequent reduction treatment with hydrogen were varied. The overall procedure is described in an earlier paper,<sup>3</sup> and the particular parameters for each alloy are given in Table I. In general, one expects larger dislocation densities and smaller AlN particles to be produced the larger is the ratio of ammonia to hydrogen in the nitrogenating atmosphere. The subsequent hydrogen reduction treatment, when employed, may be expected to reduce the dislocation density that had been produced during nitrogenation; the higher the temperature of reduction, the larger should be the loss of dislocations. The changes in nitrogen content corresponding to changes in the nitrogen activity of the gas phase were measured gravimetrically at 500°C, and the resulting isotherms are shown in Fig. 1. It is important to note that gravimetric densities of nitrogenated alloys have been measured<sup>3</sup> and were found to correspond closely with those calculated for two-phase alloys (AlN plus ferrite) without microcracks. Therefore we do not expect to observe any appreciable uptake of nitrogen or of hydrogen on internal surfaces or in the volumes of voids.

Table I. Alloy Preparation and Reference to Figures of Experimental Data

Alloy	Prior Cold Work	Composition of Nitrogenating Atmosphere*		Hydrogen Reduction Treatment		Figure No. For		
		Pct NH <sub>3</sub>	Pct H <sub>2</sub>	Temp, °C	Time, hr	Nitrogen Isotherm, 500°C	Hydrogen Isotherm	Hydrogen Isobar, 24.5°C
1	25%	17.5	82.5	500	209	—	3	—
2	25	18.5	81.5	none	—	1	4	6
3	25	18.5	81.5	525	66	1	—	7
4	13	27.0	73.0	500	136	1	—	7
		17.5	82.5†					
5	25	18.5	81.5	600	95	1	5	8
6	38	17-21%	bal.	500	72	1	9	—

\*All nitrogenations were conducted at 500°C on 0.028 cm thick specimens of a polycrystalline alloy in a cold-worked state. The sole exception is alloy 6, which was initially a single crystal of Fe-2 pct Al, and was cold-rolled to a thickness of about 0.05 cm before nitrogenation.

†Alloy was nitrogenated to 75 pct of saturation with the first gas mixture and nitrogenation was completed with the second mixture.

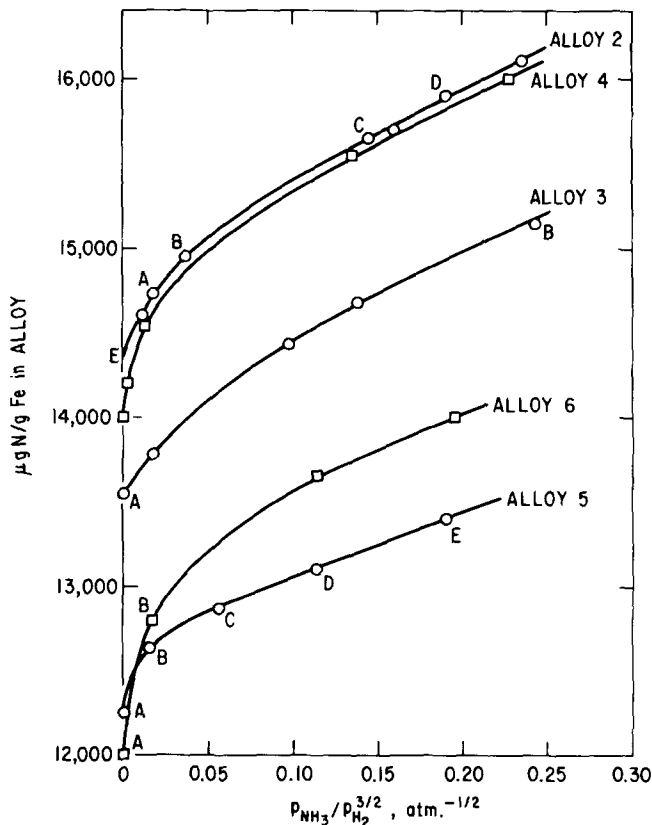


Fig. 1—Experimental reversible nitrogen absorption isotherms,  $\mu\text{g}$  nitrogen/g Fe in alloy at  $500^\circ\text{C}$ , as a function of nitrogen activity,  $a_{\text{N}} = P_{\text{NH}_3}/P_{\text{H}_2}^{3/2}$ ,  $\text{atm}^{-1/2}$ . The letters label some of the nitrogen contents at which hydrogen absorption isotherms or isobars were measured; these letters are carried through in subsequent figures. The point E for alloy 2 is an extrapolated point, the linear extrapolation being shown in Fig. 6.

### B) Hydrogenation and Hydrogen Isotherms

Establishment of an equilibrium hydrogen isotherm for an alloy of a given nitrogen content corresponding to a known nitrogen activity (at  $500^\circ\text{C}$ ) requires the measurement of the quantity of hydrogen absorbed at a measured hydrogen fugacity. The quantity of absorbed hydrogen was measured volumetrically by vacuum extraction conducted by raising the sample temperature slowly to  $300^\circ\text{C}$  over a period of a few hours. Higher extraction temperatures were also tried and were found to be unnecessary. The measurement of the hydrogen fugacity requires more extended discussion.

It was desired to measure hydrogen absorption at four hydrogen fugacities distributed over four powers of ten. In principle these fugacities, beginning at 1 atm  $\text{H}_2$ , could have been established by exposing the nitrogenated alloy to a known pressure of hydrogen gas at room temperature for a sufficient length of time to insure equilibrium. In practice, however, the equilibration times were found to be undesirably long, unless experimentally difficult surface abrasion was carried out under the hydrogen gas. For this reason, hydrogen was introduced into the alloys by cathodic charging to saturation, followed in all cases but one, by equilibration against a known pressure of hydrogen gas. Because the original cathodic charging put in a larger amount of hydrogen than those corresponding to the gas pressures to which the alloys were subsequently exposed,

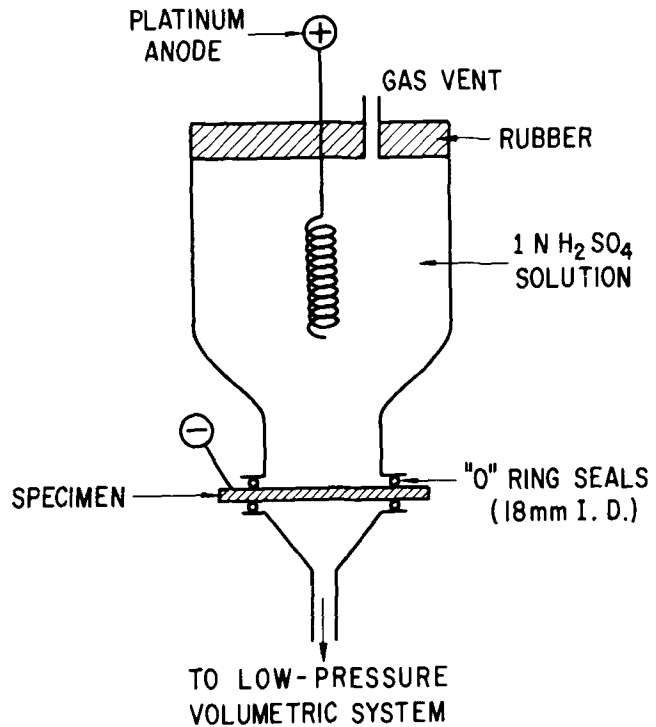
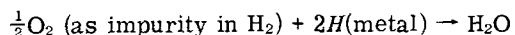


Fig. 2—Schematic diagram of cell used in the determination of hydrogen fugacity by the measurement of the steady-state permeation.

the second step involved the escape of hydrogen from the alloys. For reasons not now understood, the exiting kinetics (metal to gas) is much more rapid than the entry kinetics (gas to metal). The length of time permitted for equilibrium to be established by desorption was always in excess of 300 hr, and preferably 600 hr. In this way, the fugacities\* from 1 to 150 atm were

\*Conversion of pressure to fugacity was made by means of the fugacity coefficients of Ref. 4.

established. In one instance, a freshly degassed specimen was exposed to 1 atm of  $\text{H}_2$  gas for less than 1 hr at  $24.5^\circ\text{C}$ , during which time the specimen surface was continually abraded to facilitate the take-up of hydrogen. The amount of hydrogen absorbed was only 1 ppm below the value obtained by cathodic charging followed by desorption for 261 hr under 1 atm of  $\text{H}_2$  gas. This result makes it possible to infer that the reaction during the desorption step was part of the reversible process,  $H(\text{metal}) \rightleftharpoons \frac{1}{2}\text{H}_2(\text{g})$ , and not some irreversible process such as



Further evidence of reversibility was obtained by allowing hydrogen from a charged specimen to desorb into an atmosphere of deuterium gas. After partial desorption had occurred, the remaining hydrogen in the specimen was analyzed and was found to consist partially of deuterium. Thus, while hydrogen was leaving the specimen deuterium was entering it.

The cathodic charging was preceded by cleaning of the specimens in a solution consisting of 2 parts of 85 pct phosphoric acid and 1 part of 50 pct hydrogen peroxide. The cathodic charging itself was carried out on totally immersed specimens using 1N  $\text{H}_2\text{SO}_4$  and a current density of 2 mA per sq cm at  $24.5^\circ\text{C}$ .

Because of difficulties of carrying out equilibrations with hydrogen gas at pressures of the order of  $10^4$  atm, a different technique was used to measure the highest desired fugacity, as produced by the cathodic charging itself. To accomplish this determination, steady-state permeation rates were measured upon specially prepared diaphragms of these alloys, utilizing identical alloy compositions, surface preparation, and cathodic charging conditions at the input side of the permeation specimens as for the specimens for isotherm determinations.

The permeation cell is illustrated schematically in Fig. 2. The output side of the specimen is coated with dibutyl phthalate and abraded before assembling the permeation cell. The hydrogen escaping from the specimen at the output side is passed through a trap cooled with liquid nitrogen and is collected in a closed volumetric system where it is measured at regular time intervals. Because of the low pressure at which the gas is collected, very low permeation rates can be measured accurately. Steady-state permeation rates were presumed to have been established if the time required to reach a relatively constant rate was about equal (2 to 4 hr) to the time required for charging to saturation the specimens for the isotherm determinations. Outgassing rates of the collecting system were taken into consideration. The gas samples collected were always put through a mass spectrometer, an integral part of the system.

The permeation specimens were 0.25 and 0.50 cm thick plates of annealed Fe-2 pct Al, of which only less than 0.01 cm section of the side contacting the charging solution had been nitrogenated in the same way as had been the specimens for the isotherm determinations. The reason for using such a composite is that the very thin nitrogenated layer enables the identical charging conditions, and hence input hydrogen fugacity, to be attained as for the isotherm specimens. The flux,  $J$ , through such a composite of two media in series may be expressed as

$$J = \frac{D_1 D_2 n k_2 (f_i^{1/2} - f_o^{1/2})}{D_2 l_1 + n D_1 l_2}$$

in which  $f_i$  and  $f_o$  are the input and output hydrogen fugacities, respectively; subscripts 1 and 2 refer to the nitrogenated and unnitrogenated regions, respectively, of the composite membrane.  $n = k_1/k_2$ , where the  $k$ 's relate hydrogen fugacities to concentrations.  $D_j$  is the diffusivity of hydrogen in region  $j$ , which has the thickness  $l_j$ . Because the 2 pct Al cannot be expected to change markedly the diffusivity of hydrogen,  $D_1 \approx D_2$ . Remembering that the nitrogenated region 1 has stress fields, the solubility of hydrogen in it must be greater than in region 2 at the same hydrogen fugacity; hence  $n > 1$ . Since also  $l_2 \gg l_1$ , the above equation reduces to

$$J = D_2 k_2 (f_i^{1/2} - f_o^{1/2}) / l_2$$

which relates the observed steady-state permeation flux to the input hydrogen fugacity, which is what we wish to calculate ( $f_o = 0$  in our experiments). This relation was established by Gonzalez<sup>5</sup> for iron,\* and we

\* $D_2 k_2 = (29 \pm 0.05) \times 10^{-3} \exp(8400 \pm 400)/RT$  (Ref. 5).

apply it here to the Fe-2 pct Al solid solution because we know<sup>3</sup> that 2 pct Al changes the solubility of nitrogen only negligibly from that in annealed iron and that

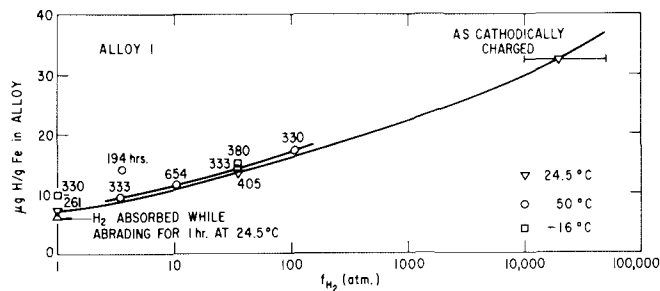


Fig. 3—Hydrogen absorption isotherms for alloy 1 at various temperatures,  $\mu\text{g}$  hydrogen/g Fe in alloy vs log fugacity of hydrogen in atm.

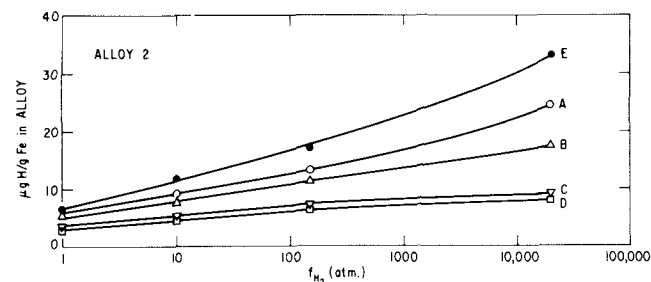


Fig. 4—Hydrogen absorption isotherms at  $24.5^\circ\text{C}$  for alloy 2 with various amounts of presorbed nitrogen designated by letters that refer to Fig. 1;  $\mu\text{g}$  H/g Fe in alloy vs log  $f_{\text{H}_2}$ , atm.

the effect upon the solubility of iron cannot be very different, and because  $D_1 \approx D_2$  as discussed above.

This technique yielded  $2 \times 10^4$  atm for the most probable hydrogen fugacity in the freshly charged specimen at  $24.5^\circ\text{C}$ ; scatter of results was from  $1 \times 10^4$  to  $5 \times 10^4$  atm. To measure the corresponding hydrogen content, the isotherm specimen was transferred from the charging solution to the extraction system within a few seconds. In the case of those specimens which after charging had been equilibrated with a hydrogen gas at known pressures, the sample and the containing pressure vessel were rapidly cooled to 78 K before releasing the hydrogen gas over the sample, prior to analysis by vacuum extraction.

The results of the measurement of hydrogen content as a function of hydrogen fugacity at various nitrogen contents, as well as of hydrogen contents as function of nitrogen contents at various hydrogen fugacities are shown in Figs. 3 to 8. In addition, some higher-temperature hydrogen isotherms, at two nitrogen contents, are shown in Fig. 9. These were obtained solely by gas equilibration. Fig. 3 shows the results of our exploratory hydrogen absorption on a nitrogenated alloy not characterized by a nitrogen isotherm. It shows the results of varying both the temperature and the durations of the equilibration step. On the basis of this exploratory work it was decided to use only  $24.5^\circ\text{C}$  for low-temperature hydrogen absorptions.

## DISCUSSION

### A) The Nitrogen Isotherms

Inspection of Fig. 1 shows that the amount of nitrogen held irreversibly (*i.e.*, at  $a_{\text{N}} = 0$ ) and also the amount of reversible nitrogen at a given value of  $a_{\text{N}}$  vary with variations in the nitrogenation treatment.

This is of course what would be expected from the different AlN particle sizes and dislocation densities produced by the different nitrogenation treatments. We have therefore the opportunity for a more intensive examination of the applicability of the Li-Chou analysis.<sup>1</sup>

We recall that this analysis considers the fact that nitrogen causes a normal strain in the  $\langle 100 \rangle$  direction in ferrite and negligible strain in other directions. Assuming a constant partial molal volume,  $\bar{V}_N$ , and using the stress field of a  $[011]$  mixed dislocation in a bcc

lattice with Burgers vector  $(a/2)[1\bar{1}\bar{1}]$ , the reversible nitrogen concentration,  $c_N$  in nitrogen atom per iron atom, is given by

$$c_N = \frac{1}{\pi r_1^2} \int_0^{2\pi} \int_0^{r_1} (c_N[100] + c_N[010] + c_N[001]) r dr d\theta \quad [1]$$

the terms in the integrand referring to the various  $\langle 100 \rangle$  directions, and in which

$$\left. \begin{aligned} c_N[100] &= \frac{(c_N^0/3) \exp \left[ -\frac{2A_N}{r} \sin \theta (2 + \cos 2\theta) \right]}{1 + (c_N^0/3) \exp \left[ -\frac{2A_N}{r} \sin \theta (2 + \cos 2\theta) \right]} \\ c_N[010] &= \frac{(c_N^0/3) \exp \frac{A_N}{r} [\sin \theta (\cos 2\theta - 2\nu) + 2\sqrt{2}(1-\nu) \cos \theta]}{1 + (c_N^0/3) \exp \frac{A_N}{r} [\sin \theta (\cos 2\theta - 2\nu) + 2\sqrt{2}(1-\nu) \cos \theta]} \\ c_N[001] &= \frac{(c_N^0/3) \exp \frac{A_N}{r} [\sin \theta (\cos 2\theta - 2\nu) - 2\sqrt{2}(1-\nu) \cos \theta]}{1 + (c_N^0/3) \exp \frac{A_N}{r} [\sin \theta (\cos 2\theta - 2\nu) - 2\sqrt{2}(1-\nu) \cos \theta]} \end{aligned} \right\} \quad [2]$$

where

$$A_N \equiv \frac{Gb\bar{V}_N}{4\pi\sqrt{3}(1-\nu)RT_N}$$

and  $2r_1$  is the mean distance between dislocations,  $r$  and  $\theta$  are cylindrical coordinates the axis of which contains the dislocation with  $\theta = 0$  along  $[100]$ ,  $c_N^0$  is the normal lattice solubility at activity  $a_N$ ,  $G$  and  $\nu$  are the shear modulus and the Poisson ratio of the lattice,  $b$  the magnitude of the Burgers vector  $= \sqrt{3} \times a/2$ ,  $a$  being the lattice parameter,  $R$  is the gas constant, and  $T_N$  is the temperature at which the isotherm was determined, 773 K in this work. From former work,<sup>1</sup>  $a_N$  and  $c_N^0$  are related at 773 K by  $a_N = 140c_N^0$ , and the activity is related to the pressures of ammonia and hydrogen according to  $a_N = P_{NH_3}/P_{H_2}^{3/2}$ , atm<sup>-1/2</sup>. A merit of the Li-Chou analysis is that the use of the

Fermi-Dirac statistics eliminates the mathematical difficulty of infinite stress at  $r = 0$  and also the need for an empirical or ad hoc energy of interaction of solute at the dislocation core. Consequently, only one adjustable parameter,  $r_1$ , remains for fitting the data. The dislocation density,  $\rho$ , is related to  $r_1$  by  $\rho = (2r_1)^{-2}$ .

These equations have been solved by computer for various values of  $r_1$  using  $G = 7.95 \times 10^{11}$  dyne per sq cm, and  $\bar{V}_N = 5.90$  cu cm per mol,  $\nu = 0.3$ . The results are shown in Fig. 10, along with the experimental curves. We note that there is a variety of goodness of agreement between the courses of the experimental curves and the course of the theoretical curves. The best agreement is that shown by alloy 5, which follows the theoretical curve for  $r_1 = 31b$ . It is perhaps significant that this alloy underwent the most drastic hydrogen reduction treatment, and that the alloy for which Li and Chou<sup>1a</sup> found excellent concordance with theory also had undergone severe hydrogen reduction. In general there is better agreement at the higher range of  $c_N^0$ , where the order of increasing nitrogen contents is that

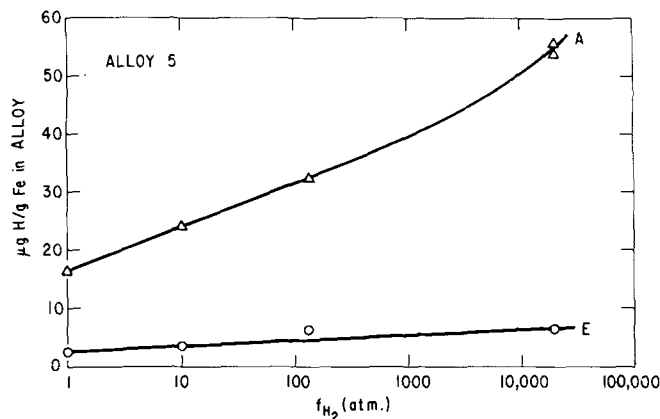


Fig. 5—Hydrogen absorption isotherms at 24.5°C for alloy 5 with two different amounts of presorbed nitrogen designated by letters that refer to Fig. 1;  $\mu\text{g H/g Fe}$  in alloy vs  $\log f_{H_2}$ , atm.

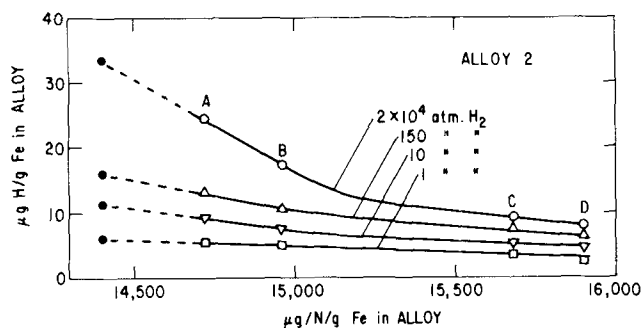


Fig. 6—The variation of hydrogen absorbed at 24.5°C and at various hydrogen fugacities with the amount of presorbed nitrogen for alloy 2,  $\mu\text{g H/g Fe}$  in alloy vs  $\mu\text{g N/g Fe}$  in alloy.

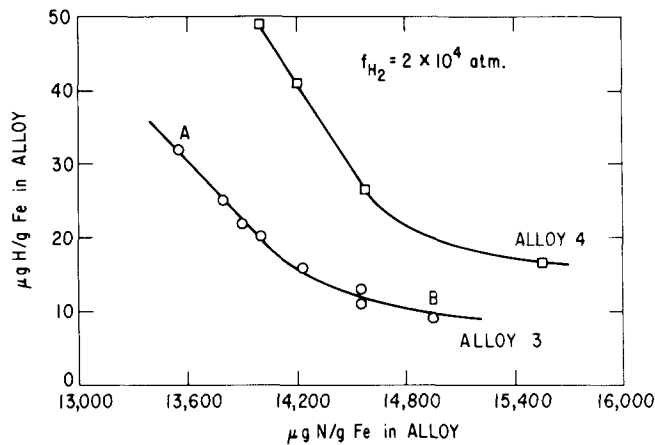


Fig. 7—The variation of hydrogen absorbed at 24.5°C and at  $f_{H_2} = 2 \times 10^4$  atm with the amount of presorbed nitrogen for alloys 3 and 4,  $\mu\text{g H/g Fe}$  in alloy vs  $\mu\text{g N/g Fe}$  in alloy.

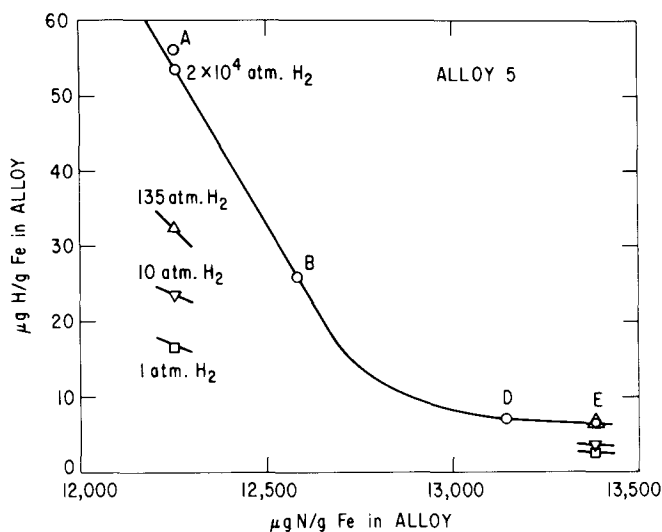


Fig. 8—The variation of hydrogen absorbed at 24.5°C and at various hydrogen fugacities with the amount of presorbed nitrogen for alloy 5,  $\mu\text{g H/g Fe}$  in alloy vs  $\mu\text{g N/g Fe}$  in alloy.

of increasing dislocation densities as expected from the preparative treatments.

If we assume for the moment that the agreement between the experimental isotherm for alloy 5 and theory is meaningful, we must try to understand the deviations from the model of the data in the low-activity range for the other alloys. From this point of view, the amount of nitrogen taken up by dislocations at low activities, and consequently at the higher-energy ( $\gamma \rightarrow 0$ ) sites is smaller than the model demands. This could be understood if the treatment accorded to the deviant alloys were such as to cause other solutes to block the high-energy sites, or else somehow decrease the number of high-energy sites without destroying the low-energy sites. To evaluate this interpretation we consider alloys 2, 3, and 5, all of which were identically nitrogenated but which differ in that alloy 2 was not hydrogen-treated, 3 was hydrogen treated at 525°C, and 5 was hydrogen-treated at 600°C. We see then that the above interpretation demands that a 525°C reduction produce blocking of high-energy sites which are accessible at dislocations in the unreduced alloy, but that a 600°C reduction makes accessible high-energy dislo-

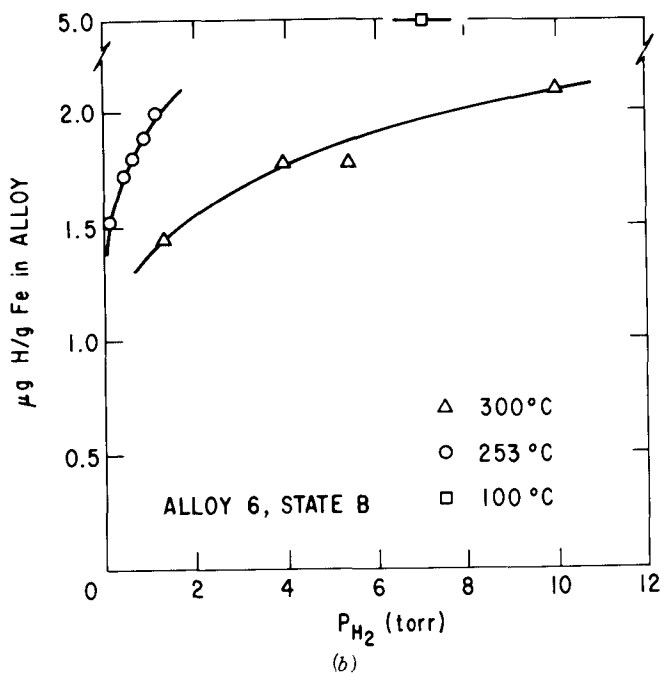
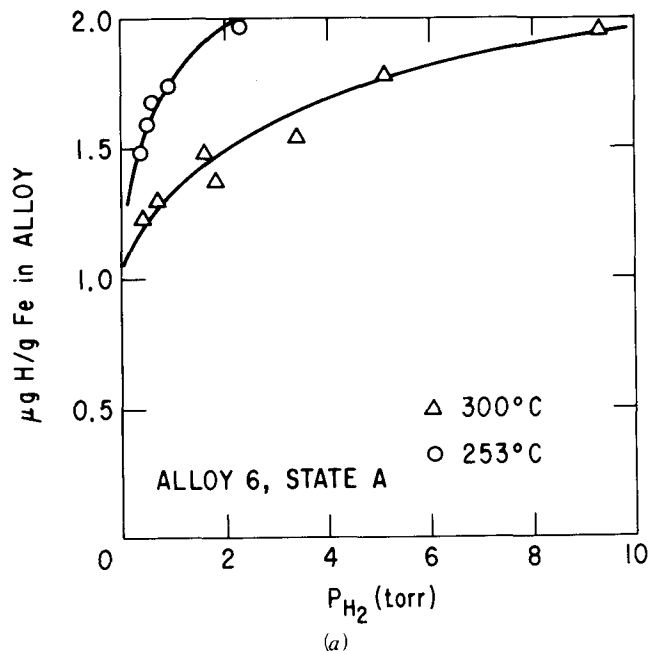


Fig. 9—Higher-temperature hydrogen isotherms for alloy 6,  $\mu\text{g H/g Fe}$  in alloy vs hydrogen gas pressure in torr. (a) Alloy 6 at state given by point A of Fig. 1. (b) Alloy 6 at state given by point B of Fig. 1.

cation sites which are blocked in the unreduced alloy. We cannot conceive of any physical process that may reasonably be expected to accompany a hydrogen reduction that will produce these conflicting demands.

We now examine the contrary assumption that the agreement between the data for alloy 5 and the predictions of the model is only fortuitous, and that there are sites for taking up nitrogen in excess of the normal lattice solubility other than at dislocations, and that such sites are contributing at low activities to the isotherm of alloy 5. We are led to explore this possibility by the knowledge of the adsorption of nitrogen at the AlN-ferrite interface. This adsorption, which occurs

during the original nitrogenation of the alloy, we have termed<sup>1</sup> irreversible since the adsorbed nitrogen remains through a 500°C hydrogen reduction, though it can undergo isotope exchange. Nevertheless, the present work shows that the reduction treatment does decrease the nitrogen held at  $a_N = 0$  from 14.4 mg N per g Fe for alloy 2 (see extrapolated isotherm in Fig. 1) to 13.5 for alloy 3 after the 525°C hydrogen treatment, and to 12.3 for alloy 5 after the 600°C hydrogen treatment.\* This behavior is consistent with the coars-

\*Indeed, later experiments have shown that the nitrogen adsorbed on AlN-ferrite interface during the original nitrogenation can be extensively removed by prolonged hydrogen reduction at 650°C, and that subsequently large quantities of nitrogen can be reversibly adsorbed at 575°C. Nevertheless, we will retain the word "irreversible" to designate the nitrogen adsorbed at the AlN-ferrite interface during the original nitrogenation.

ening of the AlN particles, and the accompanying loss of interfacial area, that may be expected to occur at high temperatures. But we note also that the 600°C reduction treatment causes alloy 5 to have a considerably larger capacity for excess hydrogen, Fig. 5, than have the other alloys. Hence, we suggest that the higher-temperature hydrogen treatment permits not only a diminution in area of the as-produced AlN-ferrite interface, but also a rearrangement of a fraction of that area to produce a lower-energy interface that can subsequently adsorb nitrogen (and hydrogen) but at reduced interaction energies. Hence this nitrogen contributes to the reversible isotherm.

In this view, the experimental isotherms of alloys 2 and 3 exhibit primarily the reversible adsorption of nitrogen upon dislocations, whereas alloy 5 has some contribution from reversible adsorption at a modified interface. It remains then to explain the negative deviation of the experimental isotherms, other than that of alloy 5, from the model employed.

In this connection it is important to point out that the model predicts very large solute concentrations at the dislocation core, so that the major contribution to the amount of nitrogen associated with one dislocation arises from the core region. In this region we can reasonably expect that the space between iron atoms at which nitrogen atoms can be accommodated is larger than in good lattice far from a dislocation. Consequently,  $\bar{V}_N/N_0$ ,\* which is the volume increase of the

\* $N_0$  = Avogadro's number.

body as a whole consequent to introducing one atom of nitrogen must be smaller at the dislocation core than in the rest of the lattice. In addition, a consequence of a large interstitial solute concentration in a given region of a lattice is that a still vacant interstitial site is made larger than it would be in an initially solute-free region, so that  $\bar{V}_N/N_0$  for the next solute atom to be introduced will be smaller than normal.

For these reasons then, a rigorous application of the thermodynamics of stressed bodies demands knowledge of  $\bar{V}_N$  as a function of position about structural singularities as well as of local solute concentration.\*

\*The question of the stress relaxation produced by the solute atom is another question still, that is not considered in the thermodynamic theory.<sup>2</sup> This point is being currently considered by N.P. Louat formerly of this Laboratory, who finds that considerable stress relaxation occurs near a dislocation core, leading to a smaller concentration of solute than predicted by the first-order thermodynamic theory.<sup>7</sup> Probably this effect can also be subsumed by using a smaller-than-normal partial molal volume.

Lacking such knowledge, we may arbitrarily assign a

partial molal volume  $\beta\bar{V}_N$  ( $\beta < 1$ ) to nitrogen occupying sites at distances  $r \leq \alpha b$  where  $\alpha \leq 1$ , letting the normal partial molar volume (*i.e.*,  $\beta = 1$ ) apply for  $r > \alpha b$ . Eqs. [1] and [2] were modified to consider the two values of partial molal volume of nitrogen in the two ranges of  $r$ . Clearly, this change produces a three-parameter model ( $r_1, \alpha, \beta$ ) and it does not seem worthwhile to adjust these back and forth until best fit with experiment is obtained. Keeping in mind that our purposes are to ascertain whether or not a two-partial molal volume model gives qualitatively better fit than the original model, and to use the values of  $r_1, \alpha$ , and  $\beta$  that reasonably describe the nitrogen data to describe the hydrogen absorption data, we solved the equations only for the cases  $\beta = 0.5, \alpha = 1$  and  $\beta = 0.4, \alpha = 0.7$ . Both calculations show better fit to the isotherms for alloys 2, 3, and 4 than that shown in Fig. 10 for the one- $\bar{V}$  model, the  $\beta = 0.4, \alpha = 0.7$  choice yielding the better fit of the two and being shown in Fig. 11. The best fit values of  $r_1$  obtained represent very large dislocation densities; for example,  $r_1 = 30b$  is equivalent to  $\rho = 5 \times 10^{11} \text{ cm}^{-2}$ . Electron microscopic observation of these specimens shows that this magnitude of dislocation density is reasonable but a more quantitative comparison is precluded by the large density, at which quantitative counting is nearly impossible.

The only conclusion that can be drawn from this exercise is that the results are consistent with the physically reasonable idea of a smaller concentration of solute at the dislocation core, than naively expected, because of the smaller  $\bar{V}$  there. However, there still remain negative deviations of the data from the two- $\bar{V}$  model at low activities for alloys 2, 3, and 4, the magnitudes of which depend somehow on the alloy preparation. Of probably greater importance to explain these discrepancies than deficiencies of the model is the possibility of a small contribution from reversible adsorption at the unmodified AlN-ferrite interface. To avoid such experimental complications one would have to produce in a metal a very large dislocation density

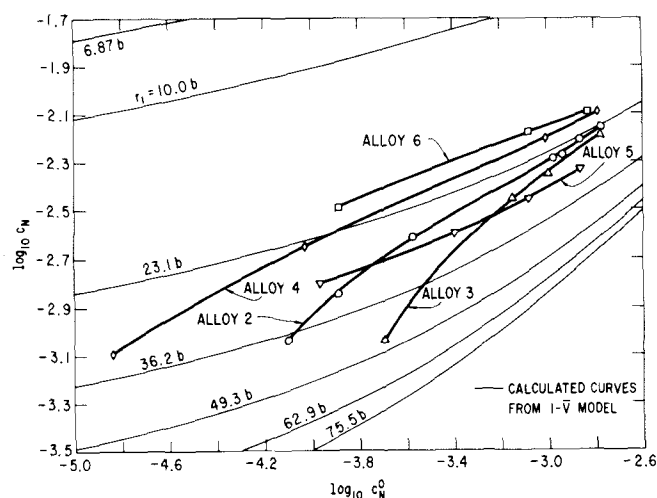


Fig. 10—Nitrogen isotherms calculated from the one-partial molal volume model for various assumed values of  $r_1$ , the mean dislocation spacing. The experimental curves of absorption of reversible nitrogen are superimposed.  $c_N^0$  is the normal lattice solubility of nitrogen at 500°C in equilibrium with the nitrogen activity in the gas phase. Units of concentrations are atom ratio N/Fe.

without the concomitant presence of either void surfaces or solid-solid interfaces.

### B) The Hydrogen Isotherms

Inspection of Figs. 3 to 8 shows that these nitrogenated alloys can absorb hydrogen reversibly at room temperature, the amount increasing with increasing hydrogen gas fugacity and decreasing with increasing amount of preabsorbed nitrogen. We see also that for alloys 2, 3, and 4 the order of increasing amount of hydrogen absorbed is also the order of increasing amount of nitrogen absorbed, and that the slopes of the curves, Figs. 6 and 7, of amount of hydrogen vs amount of nitrogen are about the same at a given hydrogen fugacity. On the other hand alloy 5, for which we had to postulate a modified interface available for reversible adsorption of nitrogen, exhibits a much larger slope, Fig. 8, for the replacement of nitrogen by hydrogen. This is consistent with the possibility that hydrogen can adsorb at interface sites vacated by reversible nitrogen. Moreover, the result shown in Fig. 8 for the hydrogen fugacity of  $2 \times 10^4$  atm is consistent with the absence of appreciable void volume that was indicated by the density measurements, since if there were appreciable void volume, presorbing of nitrogen could not have extinguished to such a marked degree the capacity of the void volume for absorbing molecular hydrogen.

In order to estimate how much of the observed absorption of hydrogen is due to dislocations and how much to interfaces it is necessary to make calculations based upon the Li-Chou analysis for the absorption of interstitial solutes about dislocations, but modified by the assumption that hydrogen can occupy only interstitial sites that are not already occupied by nitrogen. This model leads to the following equations:

$$c_H = \frac{1}{\pi r_1^2} \left\{ \int_0^{ab} \left[ \int_0^{r_1} (c_H'[100] + c_H'[010] + c_H'[001]) r dr \right] d\theta \right. \\ \left. + \int_{ab}^{r_1} (c_H''[100] + c_H''[010] + c_H''[001]) r dr \right\} \quad [3]$$

in which

$$c_H'[100] = \frac{(c_H^0/3) \exp \left[ -\frac{2A_H'}{r} f_1(\theta) \right]}{1 + \frac{(c_H^0/3) \exp \left[ -\frac{2A_H'}{r} f_1(\theta) \right]}{1 - c_N'[100]}} \\ c_H'[010] = \frac{(c_H^0/3) \exp \left[ \frac{A_H'}{r} f_2(\theta) \right]}{1 + \frac{(c_H^0/3) \exp \left[ \frac{A_H'}{r} f_2(\theta) \right]}{1 - c_N'[010]}} \\ c_H'[001] = \frac{(c_H^0/3) \exp \left[ \frac{A_H'}{r} f_3(\theta) \right]}{1 + \frac{(c_H^0/3) \exp \left[ \frac{A_H'}{r} f_3(\theta) \right]}{1 - c_N'[001]}} \quad [4]$$

with a corresponding set of equations for the three  $c_H''$  terms in which appear  $A_H''$  in place of  $A_H'$  and  $c_H''$  in place of  $c_H'$ . The  $c_N'$ 's are given by the same expressions used in Eq. [1] for the two- $\bar{V}$  model. For the sake of completeness we write them here:

$$c_N'[100] = \frac{(c_N^0/3) \exp \left[ -\frac{2A_N'}{r} f_1(\theta) \right]}{1 + (c_N^0/3) \exp \left[ -\frac{2A_N'}{r} f_1(\theta) \right]} \\ c_N'[010] = \frac{(c_N^0/3) \exp \left[ \frac{A_N'}{r} f_2(\theta) \right]}{1 + (c_N^0/3) \exp \left[ \frac{A_N'}{r} f_2(\theta) \right]} \\ c_N'[001] = \frac{(c_N^0/3) \exp \left[ \frac{A_N'}{r} f_3(\theta) \right]}{1 + (c_N^0/3) \exp \left[ \frac{A_N'}{r} f_3(\theta) \right]} \quad [5]$$

with a corresponding set of equations for the three  $c_N''$  terms in which appear  $A_N''$  in place of  $A_N'$ . In addition,

$$A_H' = \frac{Gb\bar{V}_H}{4\pi\sqrt{3}(1-\nu)RT_H}; \quad A_H'' = \frac{Gb\beta\bar{V}_H}{4\pi\sqrt{3}(1-\nu)RT_H} \\ A_N' = \frac{Gb\bar{V}_N}{4\pi\sqrt{3}(1-\nu)RT_N}; \quad A_N'' = \frac{Gb\beta\bar{V}_N}{4\pi\sqrt{3}(1-\nu)RT_N}$$

The  $f(\theta)$  are the angular functions for the stress fields of the mixed dislocation described in an earlier section and are given by

$$f_1(\theta) = \sin \theta(2 + \cos 2\theta) \\ f_2(\theta) = \sin \theta(\cos 2\theta - 2\nu) + 2\sqrt{2}(1-\nu) \cos \theta \\ f_3(\theta) = \sin \theta(\cos 2\theta - 2\nu) - 2\sqrt{2}(1-\nu) \cos \theta$$

Eq. [3] was solved by computer for  $T_H = 297.6$  K,  $\bar{V}_H = 2.0$  cm<sup>3</sup>/mol.<sup>8,9</sup> The normal lattice solubility,  $c_H^0$ , of hydrogen is related to the hydrogen fugacity,  $f_{H_2}$ , according to<sup>10</sup>

$$c_H^0 = 2.36 f_{H_2}^{1/2} \exp(-6500/RT), \text{ atom H/atom Fe} \quad [6]$$

The solution was carried out for each of two models, the one- $\bar{V}$  model ( $\alpha = \beta = 1$ ) and the two- $\bar{V}$  model ( $\alpha = 0.7, \beta = 0.4$ ), in each case using the value of  $r_1$  developed from the best fit to the experimental nitrogen isotherms of the relevant calculated curve. Thus, there are no adjustable parameters in the calculation of the hydrogen isotherms from the model, since the parameters employed are those developed from the nitrogen data. It should be noted also that using the same value of  $\beta$  for hydrogen as for nitrogen embodies the assumption that the same relative decrease of  $\bar{V}_H$  near the dislocation core occurs as for  $\bar{V}_N$ .

In Fig. 12 are shown the hydrogen isotherms for alloy 2 at zero reversibly held nitrogen ( $a_N = 0$ ) calculated from the two models and using the values of  $r_1$  developed from the nitrogen isotherms. Note that both models give agreement with experiment to within a factor of about five, with the one- $\bar{V}$  model yielding better agreement. For alloys 3 and 4 also fair agreement, especially with the one- $\bar{V}$  model, is found between theory and experiment for the amounts of hydrogen absorbed in the absence of reversibly held nitrogen. This may be seen in Figs. 14 and 15 in which the points at the lowest total nitrogen content correspond to  $a_N = 0$ . Although agreement of the calculated hydrogen absorptions with experiment is better with the one- $\bar{V}$  model, the agreement between the calculated nitrogen isotherms and experiment is worse for the one- $\bar{V}$  model. We are inclined therefore to emphasize more the two- $\bar{V}$  model and to regard the greater disagreement in the

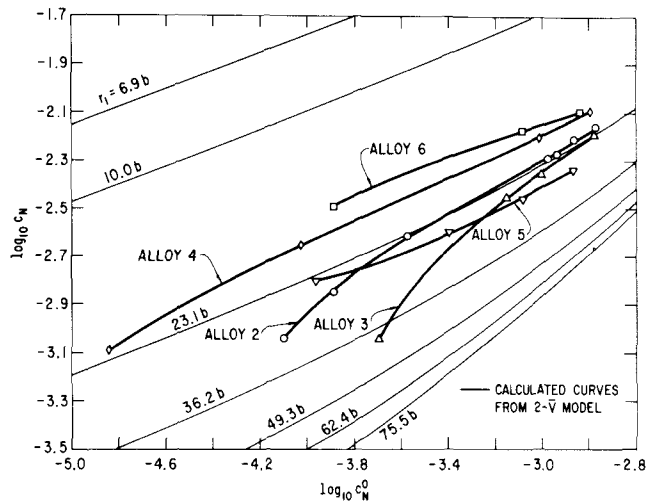


Fig. 11—Nitrogen isotherms calculated from the two-partial molal volume model ( $\beta = 0.4$ ;  $\alpha = 0.71$ ) for various values of  $r_1$ . Units of concentration are atom ratio N/Fe.

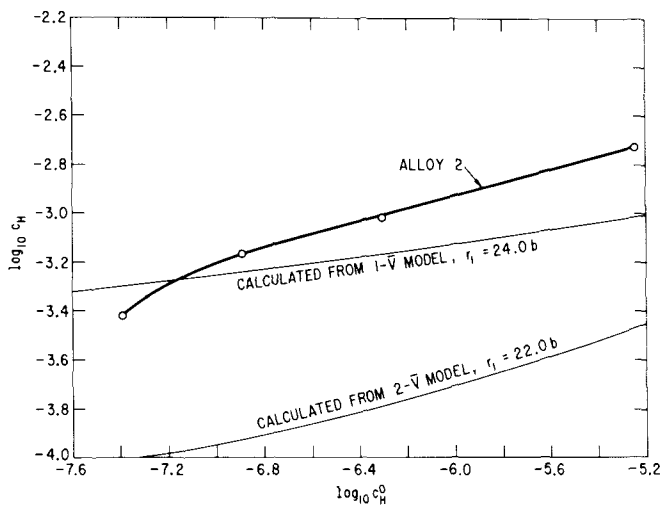


Fig. 12—Experimental hydrogen absorption isotherms at 24.5°C at zero content of reversible nitrogen compared with curves calculated from the one-partial molal volume ( $\beta = 1$ ) and two-partial molal volume ( $\beta = 0.4$ ) models with values of  $r_1$  obtained from the corresponding nitrogen isotherms. Concentrations are expressed in atom H/atom Fe.  $c_H^0$  is the normal lattice solubility of hydrogen from Eq. [6].

calculated hydrogen absorptions (at  $a_N = 0$ ) as signifying interferences from interface adsorption of hydrogen, a phenomenon which is more predominant in alloy 5.

We see in Figs. 13 to 15 that the curves, calculated from the idea that occupancy of an interstitial site by nitrogen precludes its occupancy by hydrogen, drop off much more steeply and reach lower levels of hydrogen than do the experimental curves. The idea of mutual exclusion from one site is difficult to fault, but it appears reasonable to suppose that the effect of mutual exclusion is partially overcome by an attractive interaction between the dissolved nitrogen and hydrogen atom. Such an attraction might arise, for example, if the tensile stress field into which a hydrogen is inserted adjacent to a nitrogen is increased by the nitrogen by a larger factor than the  $\bar{V}_H$  at that site is decreased by the nitrogen.

The results for alloy 5, Fig. 8, can be understood

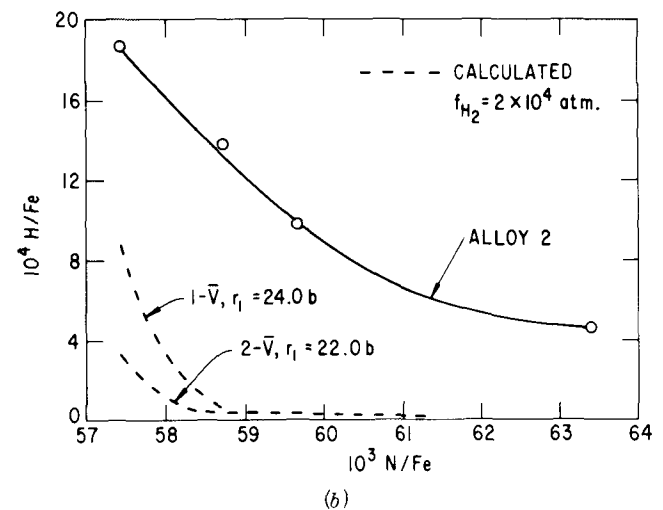
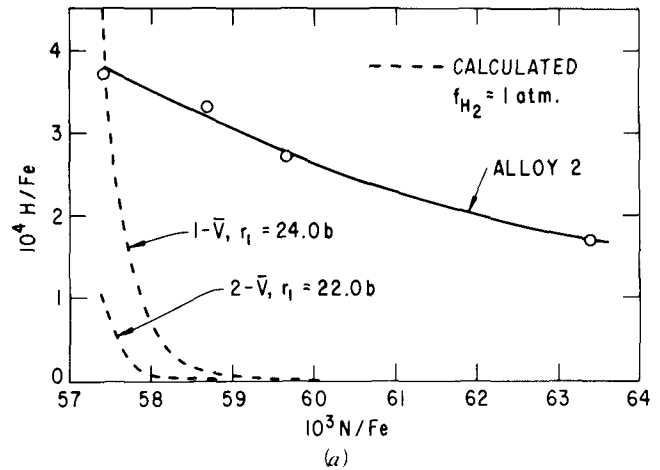


Fig. 13—Experimental hydrogen absorption at 24.5°C as a function of total nitrogen content for alloy 2, compared with curves calculated from models with parameters developed from the nitrogen isotherms. The concentrations are expressed in atom ratios. (a) Hydrogen fugacity = 1 atm. (b) Hydrogen fugacity =  $2 \times 10^4$  atm.

qualitatively in terms of the lower-energy AlN-ferrite interface that was inferred from the nitrogen isotherm for this alloy. Just as this interface, taken to have been produced by the 600°C hydrogen treatment, can reversibly adsorb nitrogen at 500°C, it can also reversibly adsorb hydrogen at 24.5°C, but only at sites not preempted by preadsorbed nitrogen. Fig. 8 then shows the blocking by nitrogen of surface sites against being filled by hydrogen, the contribution from the dislocations being less important.

High-temperature absorption isotherms for hydrogen are shown in Fig. 9 for alloy 6. A heat of absorption, relative to the gas phase, of about -25 kcal per mole  $H_2$  can be estimated from these data, and it is approximately insensitive to the presence or absence of preadsorbed reversible nitrogen. The magnitude of the energy makes it clear that this absorption cannot be related to dislocations, but must relate to adsorption at the AlN-ferrite interface. It is very difficult, however, to judge the relevance of this result to the room-temperature adsorption of hydrogen, since kinetic factors may impede the adsorption observed at high temperature from proceeding at the lower temperature.



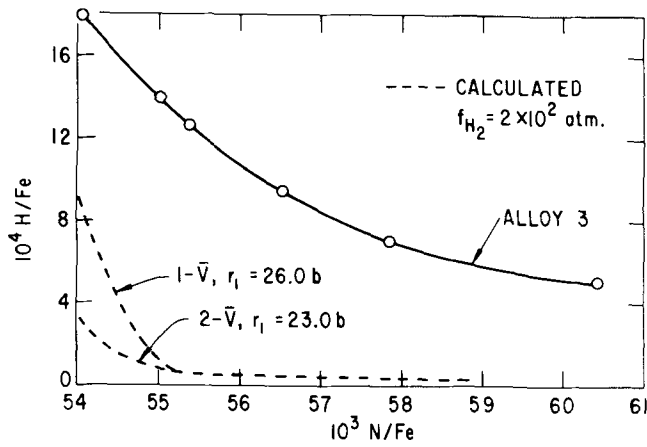


Fig. 14—Experimental hydrogen absorption at 24.5°C and  $f_{H_2} = 2 \times 10^2$  atm as a function of total nitrogen content for alloy 3, compared with curves calculated from models with parameters developed from the nitrogen isotherms. The concentrations are expressed in atom ratios.

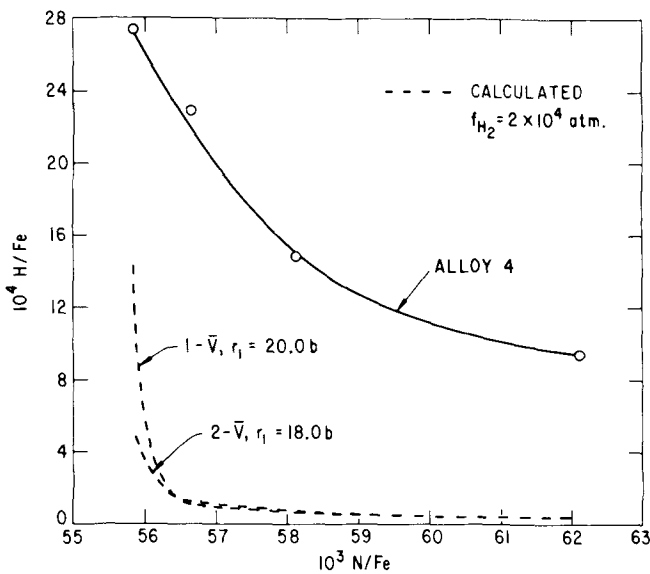


Fig. 15—Experimental hydrogen absorption at 24.5°C and  $f_{H_2} = 2 \times 10^4$  atm as a function of total nitrogen content for alloy 4, compared with curves calculated from models with parameters developed from the nitrogen isotherms. The concentrations are expressed in atom ratios.

### CONCLUSIONS

Different nitrogenation conditions and/or different conditions for subsequent hydrogen treatment can produce not only different average dislocation densities

and different extents of AlN-ferrite interface at which nitrogen is irreversibly adsorbed but also a modified interface at which nitrogen is reversibly adsorbed. In the cases where the extent of modified interface is negligible, a two- $\bar{V}$  model for dislocation-solute interaction, derived from the thermodynamics of stressed bodies, adequately describes the experimental nitrogen isotherms and with the same parameters also roughly describes the hydrogen isotherms in the absence of preadsorbed, reversible nitrogen. For such cases, however, the mutual-exclusion model fails to describe the experimentally observed decrease of hydrogen absorption at dislocations as the amount of preadsorbed nitrogen is increased. This failure is ascribed to the existence of attractive interactions between nitrogen and hydrogen which were not considered by the model, though it may be due to other causes. The modified AlN-ferrite interface can reversibly (at 500°C) adsorb nitrogen and can reversibly (at 24.5°C) adsorb hydrogen at sites not occupied by nitrogen, whereas the "unmodified" interface does not do so to an appreciable extent. These results suggest complexity in the behavior of internal interfaces with respect to trapping of hydrogen, relevant to the interpretation of the diffusion and solubility of hydrogen in steels.<sup>11</sup>

### ACKNOWLEDGMENT

The experimental work of this investigation was carried out by R. M. Lytle and F. N. Davis. We are grateful to B. E. Sundquist for carrying out the computer solutions of the equations.

### REFERENCES

1. H. H. Podgurski, R. A. Oriani, and F. N. Davis: *Trans. TMS-AIME*, 1969, vol. 245, p. 1603.
- 1a. J. C. M. Li and Y. T. Chou: Appendix to Ref. 1.
2. J. C. M. Li, R. A. Oriani, and L. S. Darken: *Z. Physik. Chem. (N.F.)*, 1969, vol. 49, p. 271.
3. H. H. Podgurski and H. E. Knechtel: *Trans. TMS-AIME*, 1969, vol. 245, p. 1595.
4. C. E. Holley, W. J. Worther, and R. K. Zeigler: Los Alamos Report No. 2271.
5. O. D. Gonzalez: *Trans. TMS-AIME*, 1969, vol. 245, p. 607.
6. H. A. Wriedt and L. Zwell: *Trans. TMS-AIME*, 1962, vol. 224, p. 1242.
7. N. P. Louat: formerly of E. C. Bain Laboratory; presently at Battelle Memorial Institute, Columbus, Ohio, private communication.
8. R. A. Oriani: *Trans. TMS-AIME*, 1966, vol. 236, p. 1368.
9. H. Wagenblast and H. A. Wriedt: *Met Trans.*, 1971, vol. 2, p. 1393.
10. O. D. Gonzalez: private communication, quoted by R. A. Oriani, *Proc. Conf., Fundamental Aspects of Stress Corrosion Cracking*, Columbus, 1967, N.A.C.E., (1969) p. 32.
11. R. A. Oriani: *Acta Met.*, 1970, vol. 18, p. 147.